Available online at www.sciencedirect.com

SCIENCE DIRECT®

Journal of the European Ceramic Society 23 (2003) 1277–1282

www.elsevier.com/locate/jeurceramsoc

Effect of grinding on the leaching behaviour of pyrophyllite

J. Temuujin[a], K. Okada[b], T.S. Jadambaa[c], K.J.D. MacKenzie[d,*], J. Amarsanaa[c]

[a]*Institute of Chemistry and Chemical Technology, Mongolian Academy of Sciences, Ulaanbaatar 51, Mongolia*
[b]*Department of Metallurgy and Ceramics Science, Tokyo Institute of Technology, O-okayama, Meguro-ku, Tokyo, Japan*
[c]*Department of Chemical Technology, Science and Technological University of Mongolia, Ulaanbaatar 46, Mongolia*
[d]*New Zealand Institute for Industrial Research and Development, Lower Hutt, New Zealand*

Received 28 April 2002; received in revised form 6 August 2002; accepted 19 August 2002

Abstract

The effect of dry grinding on the leaching behaviour of pyrophyllite has been studied by XRD, FT-IR, thermal analysis and N_2 adsorption techniques. Pyrophyllite samples were ground for 3, 6, 12 and 18 h. Grinding initially causes the surface area of the pyrophyllite to increase to ~73 m^2 g^{-1}, decreasing with longer grinding because of particle agglomeration. Leaching the ground pyrophyllite with 4 M HCl at 80 °C for 2 h causes depletion of Al^{3+} and increases the surface area. The highest surface area was recorded in the leached sample ground for 3 h (156.9 m^2 g^{-1} with a pore volume of 0.36 ml g). Structural breakdown by grinding is thought to be the main reason for the enhanced leaching behaviour of the pyrophyllite, but grinding for extended periods decreases the leaching rate without enhancement of the porous properties.

Keywords: Grinding; Leaching; Milling; Pyrophyllite

1. Introduction

The preparation of porous material from clay minerals by selective leaching involves the removal of part of the clay by treatment with acid or base, leaving pores within the clay structure. Silica with a high surface area prepared by this technique has potential practical applications as catalyst supports,[1] catalysts,[2,3] adsorbents[4] and agents for organic molecule separation.[5] Acid-activated clays are used for removing colour and other impurities from cooking oil[6] or as a component of carbonless copying papers.[7] On the basis of their leaching behaviour, clay minerals can be classified into three types according to their structure and the maximum obtainable surface area, which varies from 400 to 670 m^2 g^{-1}. However, large differences have been found in the leaching rates even in clay minerals of the same type. The greatest differences in the surface areas of the leached products have been reported in the 2:1 clay minerals (<20 m^2 g^{-1} in phlogopite[8] and 670 m^2 g^{-1} in vermiculite[9]). These large differences have been suggested[10] to be related to the chemical composition of the clay, but other factors such as the particle size and the ratio of acid to solid are also important.[9] Generally it appears that in the 2:1 clay minerals the interlayer cations are more leachable than the octahedral cations, which in turn are more leachable than the tetrahedral cations. In some 2:1 clay minerals substitution occurs of cations such as Al^{3+} and Fe^{3+} into the S–O tetrahedral layers. It appears likely that high surface areas result from the retention of the micropores formed between tetrahedral layers of the clay minerals. We have suggested[9] that simultaneous substitution of Al^{3+} and Fe^{3+} in the tetrahedral layers of the clay mineral produces silica of higher surface area than would be obtained from a mineral with only Al^{3+} substitution. This observation may be related to the slower leaching of Fe^{3+} than Al^{3+}, resulting in the stabilization of the tetrahedral silica layer and prevention of further condensation which decreases the surface area.[9]

On the other hand almost no substitution occurs in the tetrahedral layers of 2:1 clay minerals such as talc and pyrophyllite. These minerals are very resistant to acid attack,[11–13] possibly due to their unstrained structure and the presence of oxygen atoms solely between the layer surfaces.

---

* Corresponding author.
E-mail address: kenneth.mackenzie@vuw.ac.nz (K.J.D. MacKenzie).

0955-2219/03/$ - see front matter © 2002 Elsevier Science Ltd. All rights reserved.
PII: S0955-2219(02)00297-2

Distortion of the layer structure of talc by grinding significantly influences its leaching behaviour.[11] A similar improvement in the leaching behaviour might also be expected in mechanically activated pyrophyllite. The objective of the present study was to evaluate the effect of grinding on the leaching behaviour of pyrophyllite.

2. Experimental

Commercial pyrophyllite (Shokozan Mining Co., Japan) was used in this study. The producer's data indicated a particle size distribution of $90\% < 16.69$ μm, $50\% < 5.97$ μm, $10\% < 2.24$ μm and a chemical composition on a dry weight basis of $SiO_2 = 73.25\%$, $Al_2O_3 = 26.5\%$ and $Fe_2O_3 = 0.21\%$. The material contains quartz as an impurity, estimated to be about 7%. On this assumption the structural water associated with the pyrophyllite was estimated from the TG curve (Fig. 1) to be 5.2%, giving a structural composition of $(Al_{3.99}Fe_{0.02})[Si_{7.7}Al_{0.3}]O_{20}(OH)_4$ calculated on the basis of 24O. The DTA curve of this pyrophyllite (Fig. 1) shows a broad endothermic peak centered at 810 °C and small exothermic peak at 905 °C. The endothermic peak is associated with sample dehydroxylation, as shown by the TG curve. The DTA curve is similar to a published curve for pyrophyllite from North Carolina[14] which shows a broad, shallow dehydroxylation endotherm at 650–850 °C. The weight loss up to 1000 °C corrected for the quartz impurity (5.2%) is in reasonable agreement with ideal pyrophyllite (5%).

Pyrophyllite samples (2 g) were ground for 3, 6, 12 and 18 h in a planetary pot mill LA-PO.1 (Itoh Co., Japan) at room temperature. The rotation speed of the mill was 300 rpm and the milling media and pot were of corundum. Balls of 5 mm dia. were used, the weight ratio of balls to sample being 30:1. After each grinding, 1 g of sample was treated with 100 ml of 4 M HCl at 80 °C for 2 h. After leaching, 100 ml of cold distilled water was added and the sample allowed to cool for 30 min. The suspension was filtered and dried at 110 °C overnight.

XRD patterns were obtained using monochromated CuK_α radiation with a Shimadzu LabX XRD-6100 diffractometer. The chemical compositions of the samples were determined by X-ray fluorescence using a Rigaku RIX2000 spectrometer. Differential thermal analysis and thermogravimetry (DTA-TG) (Rigaku, Thermo-plus 8120) were carried out at a heating rate of 10 °C/min to 1000 °C. Infrared spectra were recorded using a Shimadzu FTIR 8200PC spectrometer with the samples suspended in KBr discs.

The specific surface area (S_{BET}) was measured by the BET method at −196 °C using nitrogen gas with a Quanta Chrome Autosorb-1 instrument. The total pore volume (V_t) was derived from the degree of adsorption at $P/P_0 = 0.999$. The pore size distribution was calculated by the BJH method using the adsorption isotherm. Particle size was estimated from the equation $D_{BET} = F/\rho \cdot S_{BET}$, where ρ is density of pyrophyllite (2.8 g/cm^3), S_{BET} the specific surface area and F a particle-shape factor ($F = 6$ for spherical particles[18]).

3. Results and discussion

3.1. X-ray diffraction

The X-ray diffraction patterns of pyrophyllite, before and after grinding for different times, are shown in Fig. 2. Grinding causes the intensity of the pyrophyllite reflections to decrease significantly but never completely

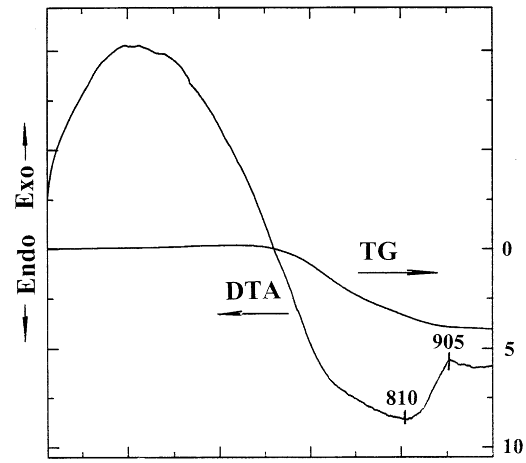

Fig. 1. DTA and TG curves of unground pyrophyllite. Heating rate 10 °C/min in air.

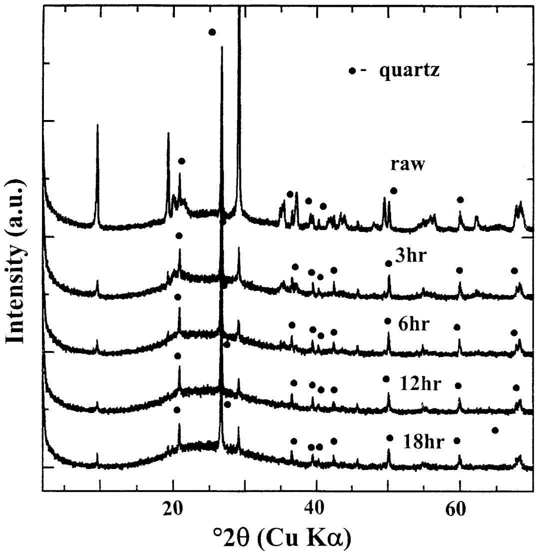

Fig. 2. XRD diffractograms of ground and unground pyrophyllite.

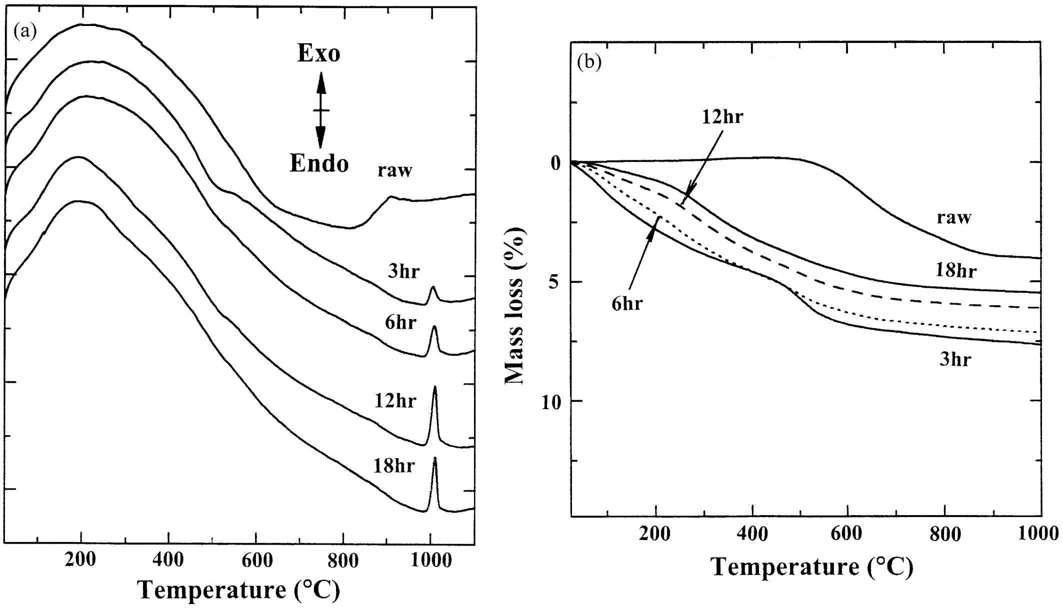

Fig. 3. Thermal analysis curves of ground and unground pyrophyllite. (a) DTA curves, (b) TG curves.

disappear. After grinding for 18 h, the major crystalline phase present is quartz, the XRD intensity of which is slightly decreased by grinding. By contrast with previous research on the grinding of pyrophyllite[15–18] we could not obtain fully amorphous material. Previous authors[15] have suggested that grinding has less effect on the non-basal XRD reflections than the basal reflections. However, the retention of the basal (001) reflection in our samples ground for 3–18 h suggests that the basal reflection may also be stable to grinding and that alteration of the crystalline structure does not necessarily occur readily along the *c*-axis of the crystal structure.

3.2. Thermal analysis

DTA and TG curves of the raw and ground samples are shown in Fig. 3. Grinding for 3 h causes the endothermic dehydroxylation peak temperature of the pyrophyllite to decrease from 550 to 490 °C, with a similar change in the TG curve. The DTA traces of the ground samples show a new exothermic peak at about 1005 °C, the intensity of which is directly related to the grinding times and also increases with longer leaching times (but reaches a plateau in the samples ground for 12 and 18 h). This peak is thought to arise from the presence of Si–O–Al linkages in the non-crystalline aluminosilicate phases occurring in the ground samples.[17,19] On the other hand, grinding increases the TG weight loss of the ground samples, especially those ground for shorter times. Grinding for 6 h causes the weight loss to become more gradual, as observed in gel-like materials.[19] The loss of hydration water from pyrophyllite occurs below 200 °C, while dehydroxylation of the ground material occurs at higher temperatures (up to 1000 °C). The observed increase in the weight of both free water and hydroxyls in the ground samples is probably due to the adsorption of atmospheric moisture and rehydroxylation. The weight loss associated with the latter decreases with increasing grinding times, possibly due to the formation of a progressively more aggregated structure which hinders the access of environmental moisture. These results are similar to those reported for ground pyrophyllite.[16]

3.3. Specific surface area and particle size analysis

Fig. 4 shows the change of S_{BET} and particle size as a function of grinding time. A large increase in the S_{BET}

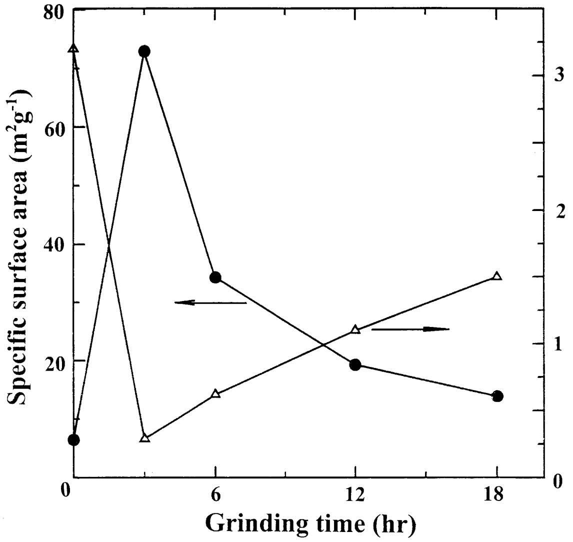

Fig. 4. S_{BET} and particle size of pyrophyllite as a function of grinding time.

value (from 6.5 to 72.9 $m^2 g^{-1}$) occurs during the first 3 h of grinding, but this value decreases to 13.87 $m^2 g^{-1}$ on grinding for 18 h. Changes in the surface areas of these samples show inverse behaviour, suggesting that the decrease in the surface area is related to particle agglomeration. The same behaviour has previously been reported in ground pyrophyllite[15–18] and imogolite.[20] This suggests that the practical limit to grinding is the point at which the particles re-aggregate.

The specific surface area of the present ground pyrophyllite is higher than reported by other workers.[15–18,21] This may be related to the quartz impurity in the present samples, the harder quartz particles producing a greater degree of structural distortion of the pyrophyllite during the initial stages of the grinding prior to aggregation. According to Henmi and Yoshinaga[20] the decrease in the surface area is related to the collapse of the micropores responsible for the initial increase of surface area resulting from the high degree of structural distortion and changes in particle morphology induced in the initial stages of grinding. This explanation also appears to be the most appropriate to the results found for the present system.

3.4. FTIR analysis

The FTIR spectra of raw, ground and leached pyrophyllite are shown in Fig. 5. Structural distortion of the original pyrophyllite by grinding causes broadening of the spectral features at 950–1200 cm^{-1} and a decrease in the intensity of the 3670 cm^{-1} band, the latter arising from the hydroxyl groups of the original pyrophyllite. After grinding, new bands due to adsorbed water appear at 3640 and 1630 cm^{-1}, their intensity decreasing with longer grinding times in agreement with the thermogravimetric data. The doublet clearly observed at 780 and 800 cm^{-1} is due to the presence of quartz.[22] The Al–OH deformation vibration at 950 cm^{-1} in the original pyrophyllite almost disappears on grinding but reappears in the leached samples, this behaviour being associated with the amorphized region of the Al–OH structure. The spectra of the samples ground for longer times and leached become similar to the spectra of amorphous silica, but retain some of the bands of the original pyrophyllite.

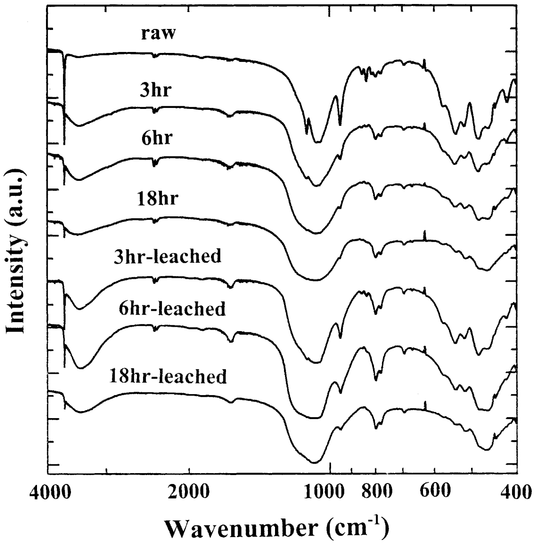

Fig. 5. FT-IR spectra of unground, ground and leached pyrophyllite samples.

The results of all the characterization experiments are consistent with increasing structural breakdown of the pyrophyllite as the grinding time is increased.

3.5. Porous properties

Table 1 shows the changes in the chemical composition and porous properties of the raw and ground pyrophyllite after leaching. The highest value of S_{BET} was shown by the sample ground for 3 h but the greatest depletion of Al^{3+} occurred after grinding for 6 h. Both S_{BET} and the depletion of Al^{3+} decreases in samples ground for longer times. On the other hand, although the depletion of Al^{3+} is similar in the samples ground for 3 and 18 h, their surface area and pore volume is considerably different, suggesting that the porous properties of the ground and leached samples are not solely dependent on cation leaching.

The DTA results suggest that an amorphous aluminosilicate Al–O–Si linkage forms to a greater extent in the sample ground for 18 h than in the 3 h ground sample. Since Okada et al. reported[23] that selective leaching of cations occurs faster in amorphized clay minerals, the leaching results do not appear to be consistent with the grinding behaviour of these samples. However, it should be remembered that in mechanically amorphized pyrophyllite the Al–O–Si bonds are formed by conversion of octahedral Al to tetrahedral coordination, the amount of tetrahedral Al increasing with prolonged grinding.[18] We have also shown that complete leaching of Al^{3+} occurs in mechanically amorphized kaolinite, which contains Al–O–Si bonds.[24] It is therefore unlikely that the presence of Al–O–Si bonds is the sole reason for the slower leaching of Al^{3+}. Another factor to be

Table 1
Chemical composition and porous properties of ground and leached pyrophyllite

Sample	SiO_2 (wt.%)	Al_2O_3 (wt.%)	Fe_2O_3 (wt.%)	S_{BET} ($m^2 g^{-1}$)	Vp (ml g^{-1})
Pyrophyllite[a]	73.25	26.5	0.21	6.8	0.04
Ground 3 h, leached	84.74	15.02	0.12	156.9	0.36
Ground 6 h, leached	91.04	8.88	0.07	156.5	0.31
Ground 12 h, leached	90.19	9.73	0.07	130.8	0.22
Ground 18 h, leached	85.94	13.94	0.11	94.06	0.15

[a] Includes quartz impurity

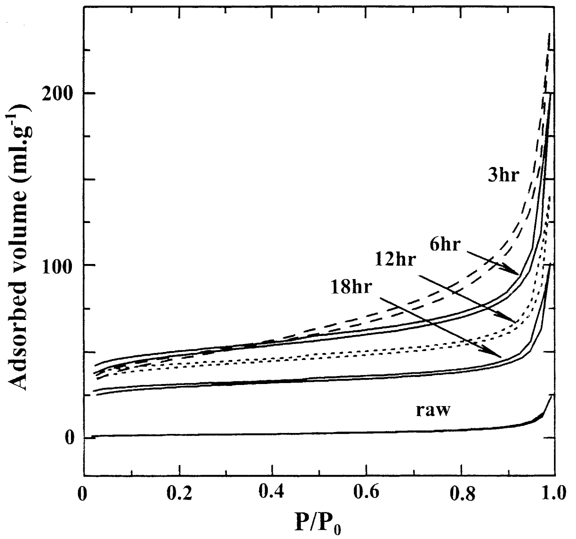

Fig. 6. N_2 adsorption isotherms of unground, ground and leached pyrophyllite samples.

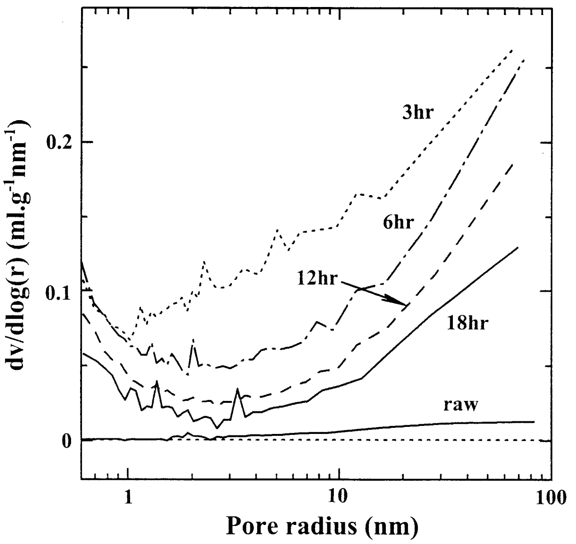

Fig. 7. Pore size distribution (PSD) curves of unground, ground and leached pyrophyllite samples.

taken into account is the surface energy of the agglomerated particle structure generated by prolonged grinding. Thus, the inhibited leaching behaviour of the sample ground for 18 h may reflect either the formation of strong Al–O–Si bonds or an agglomerated particle structure.

Fig. 6 shows N_2 adsorption isotherms of the raw, ground and leached samples. Raw pyrophyllite is non-porous, with a type II isotherm.[25] The presence of micropores in the ground and leached samples results in an isotherm with an initial portion resembling a type I isotherm but the remainder resembling a mixture of type II and type IV isotherms. These isotherms also show a hysteresis loop arising from the presence of mesopores, but with no clear closure point of the desorption isotherm and the observed low pressure hysteresis. The N_2 adsorption volume decreases in the samples ground for longer times, in agreement with their surface area and pore volume values.

The pore size distribution (PSD) curves of the raw and ground samples after leaching are shown in Fig. 7. The general trend of the PSD is similar to the N_2 adsorption isotherm, i.e. the greatest number of pores occurs in the sample ground for 3 h and leached. The total concentration of pores decreases with increased grinding time. The presence of significant numbers of micropores is suggested by the extension of the curves into the micropore region, the height of which however decreased at longer grinding times. This suggests that the observed micropores not only result from leaching of the Al from the ground samples, but also include intraparticle micropores introduced by grinding. The number of micropores decreases with increased grinding. The absence of a sharp peak from the PSD curves indicates a lack of uniform pore size distribution and microstructure.

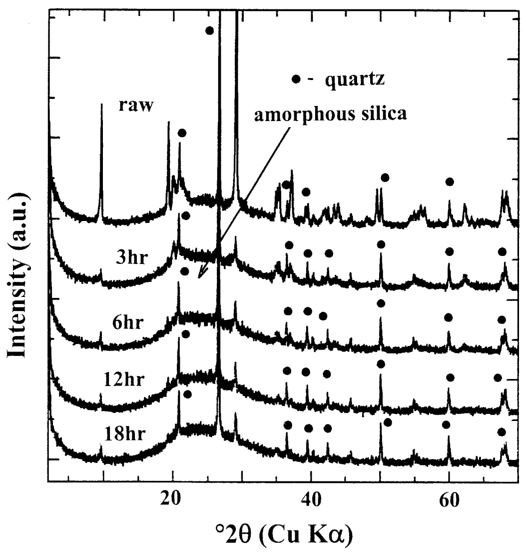

Fig. 8. XRD diffractograms of leached pyrophyllite samples.

The XRD diffraction patterns of the ground and leached samples are shown in Fig. 8. The diffraction patterns of the leached samples are similar to those of the ground samples (Fig. 2), but with an increase in the broad feature at about 20–25°2θ arising from the presence of amorphous silica. The persistence in these samples of peaks due to crystalline pyrophyllite indicates high chemical stability of this phase.

4. Conclusions

Grinding of pyrophyllite causes structural distortion with the formation of an amorphous phase containing Al–O–Si bonds. There is, however, a limit to the long-range disorder induced in pyrophyllite by grinding, with a degree of structural order persisting even after longer grinding times. Grinding introduces a significant number of intraparticle micropores. Structural breakdown of the ground pyrophyllite facilitates leaching of its Al^{3+}, but this effect diminishes at longer grinding times. Possible reasons for this behaviour include the formation of both Al–O–Si bonds and a highly agglomerated particle structure during grinding. To obtain a material of high surface area from mechanically amorphized pyrophyllite, it is necessary to determine the optimal grinding conditions.

References

1. Aznar, A. J., Gutierrez, E., Diaz, P., Alvarez, A. and Poncelet, G., Silica from sepiolite: preparation, textural properties, and use as support to catalyst. *Micropor. Mater.*, 1996, **6**, 105–114.
2. Suquet, H., Chevalier, S., Marcilly, C. and Barthomeuf, D., Preparation of porous materials by chemical activation of the Llano vermiculite. *Clay Miner.*, 1991, **26**, 49–60.
3. Corma, A. and Perez-Pariente, J., Catalytic activity of modified silicates: I. Dehydration of ethanol catalysed by acidic sepiolite. *Clay Miner.*, 1987, **22**, 423–433.
4. Gonzales, L., Ibarra, L. M., Rodriguez, A., Moya, J. S. and Valle, F. J., Fibrous silica gel obtained from sepiolite by HCl attack. *Clay Miner.*, 1984, **19**, 93–98.
5. Okada, K., Shimai, A., Hayashi, S. and Yasumori, A., Adsorption properties of microporous silica prepared from metakaolinite by selective leaching method. *Clay Sci.*, 1999, **11**, 73–82.
6. Anderson, A. J. C. and Williams, P. N., *Refining of Oils and Fats for Edible Purposes*. Pergamon, New York, 1962.
7. Fahn, R. and Fenderl, K., Reaction products of organic dye molecules with acid-treated montmorillonites. *Clay Miner.*, 1983, **18**, 447–458.
8. Kaviratna, H. and Pinnavaia, T. J., Acid hydrolysis of octahedral Mg^{2+} sites in 2:1 layered silicates: an assessment of edge attack and gallery access mechanism. *Clays Clay Miner.*, 1994, **42**, 717–723.
9. Temuujin, J., Okada, K. and MacKenzie, K. J. D., Preparation of porous silica from vermiculite by selective leaching. *Appl. Clay Sci.* (in press).
10. Harkonen, M. A. and Keiski, R. L., Porosity and surface area of acid-leached phlogopite: the effect of leaching conditions and thermal treatment. *Colloids and Surfaces*, 1984, **11**, 323.
11. Temuujin, J., Okada, K., Jadambaa, T. S., MacKenzie, K. J. D. and Amarsanaa, J., Effect of grinding on the preparation of porous material from talc by leaching. *J. Mater. Sci. Lett.* (in press).
12. Perez Rodriguez, J. L., Maqueda, C. and Justo, A., Pyrophyllite determination in mineral mixtures. *Clays Clay Miner.*, 1985, **33**, 563–566.
13. Maqueda, C., Perez Rodriguez, J. L. and Justo, A., Effect of pyrophyllite on the precipitation of aluminium sulfate during the dissolution of aluminosilicates by acid mixtures. *Analyst*, 1987, **112**, 1085–1086.
14. MacKenzie, R. C., *The Differential Thermal Investigation of Clays*. Mineralogical Society, London, 1957.
15. Perez-Rodriguez, J. L., Madrid Sanchez Del Villar, L. and Sanchez-Soto, P. J., Effects of dry grinding on pyrophyllite. *Clay Miner.*, 1988, **23**, 399–410.
16. Perez-Rodriguez, J. L. and Sanchez-Soto, P. J., The influence of the dry grinding on the thermal behaviour of pyrophyllite. *J. Thermal Anal.*, 1991, **37**, 1401–1413.
17. Sanchez-Soto, P. J., Justo, A. and Perez-Rodriguez, J. L., Grinding effect on kaolinite-pyrophyllite-illite natural mixtures and its influence on mullite formation. *J. Mater. Sci.*, 1994, **29**, 1276–1283.
18. Sanchez-Soto, P. J., Perez-Rodriguez, J. L., Sobrados, I. and Sanz, J., Influence of grinding in pyrophyllite-mullite thermal transformation assessed by ^{29}Si and ^{27}Al MAS NMR spectroscopies. *Chem. Mater.*, 1997, **9**, 677–684.
19. Temuujin, J., Okada, K. and MacKenzie, K. J. D., Characterization of aluminosilicate (mullite) precursors prepared by a mechanochemical process. *J. Mater. Res.*, 1998, **13**, 2184–2189.
20. Henmi, T. and Yoshinaga, N., Alteration of imogolite by dry grinding. *Clay Miner.*, 1981, **16**, 139–149.
21. Okuda, S., Inoue, K. and Williamson, W. O., Negative surface charges of pyrophyllite and talc. *Proc. Clay Conf. Tokyo, 1969, 31–41.*
22. Plyusnina, I. I., *Infrared Spectra of Minerals*. Moscow State University, Moscow, 1977.
23. Okada, K., Shimai, A., Takei, T., Hayashi, S., Yasumori, A. and MacKenzie, K. J. D., Preparation of microporous silica from metakaolinite by selective leaching method. *Micropor. Mesopor. Mater.*, 1998, **21**, 289–296.
24. Temuujin, J., Burmaa, G., Amgalan, J., Okada, K., Jadambaa, T. S. and MacKenzie, K. J. D., Preparation of porous silica from mechanically activated kaolinite. *J. Por. Mater.*, 2001, **8**, 247–252.
25. Sing, K. S. W., Everett, D. H., Haul, R. A. W., Moscou, L., Pierotti, R. A., Rouquerol, J. and Siemieniewska, T., Reporting physisorption data for gas/solid systems with special reference to the determination of surface area and porosity. *Pure and Appl. Chem.*, 1985, **57**, 603–619.